Laser-induced charge-disproportionated metallic state in $LaCoO_3$

M. Izquierdo,[1,2,3] M. Karolak,[3] C. Trabant,[4] K. Holldack,[4] A. Föhlisch,[4] K. Kummer,[5] D. Prabhakaran,[6] A. T. Boothroyd,[6] M. Spiwek,[7] A. Belozerov,[8,9] A. Poteryaev,[9] A. Lichtenstein,[2,3,9] and S. L. Molodtsov[2,10,11]

[1]*Synchrotron Soleil, L'Orme des Merisiers St-Aubin, BP-48, 91192, Gif-sur-Yvette, France*

[2]*European XFEL Gmbh, Albert-Einstein-Ring 19, 22761 Hamburg, Germany*

[3]*Institut für Theoretische Physik, Universität Hamburg, Jungiusstraße 9, 20355 Hamburg, Germany*

[4]*Helmholtz-Zentrum Berlin für Materialien und Energie GmbH, BESSY II, Albert-Einstein-Strasse 15, 12489 Berlin, Germany*

[5]*European Synchrotron Radiation Facility, BP 220, F-38043 Grenoble Cedex, France*

[6]*Clarendon Laboratory, Department of Physics, University of Oxford, Parks Road, Oxford OX1 3PU, UK*

[7]*Deutsches Elektronen-Synchrotron DESY, Notkestrasse 85, D-22607, Hamburg, Germany*

[8]*Institute of Metal Physics, Russian Academy of Sciences, 620990 Yekaterinburg, Russia*

[9]*Ural Federal University, 620990 Yekaterinburg, Russia*

[10]*Institute of Experimental Physics, Technische Universität Bergakademie Freiberg, 09599 Freiberg, Germany*

[11]*ITMO University, Kronverkskiy pr. 49, 197101 St. Petersburg, Russia*

Understanding the origin of the spin transition in $LaCoO_3$ is one of the long-standing aims in condensed matter physics. Aside from its fundamental interest, a detailed description of this crossover will have a direct impact on the interpretation of the semiconductor-to-metal transition (SMT) and the properties of the high-temperature metallic phase in this compound, which has shown to have important applications in environmentally friendly energy production. To date, the spin transition has been investigated mainly as a function of temperature in thermal equilibrium. These results have hinted at dynamical effects. In this paper, we have investigated the SMT by means of pump-probe soft x-ray reflectivity experiments at the O K, Co L, and La M edges and theoretical calculations within a DFT^{++} formalism. The results point towards a laser-induced metallization in which the optical transitions stabilize a metallic state with high-spin configuration and increased charge disproportionation.

PACS number(s): 78.47.−p, 71.28.+d, 71.20.−b

I. INTRODUCTION

At a time when environmental preservation and rational use of natural resources are a priority, finding materials with increased efficiency and reduced waste in energy production is one of the key subjects in materials science research. In this context, $LaCoO_3$ (LCO) and related compounds have recently gained a lot of attention due to their potential applications in various efficient, environmental-friendly energy production domains. These include (i) catalytic oxidation of volatile organic contaminants (VOCs) [1], hydrocarbons [2], CO and lean NO_x trapping (LNT) that could lead to new diesel engines [3], (ii) oxygen membranes to operate at high temperatures in oxyfuel power plants [4], (iii) fuel cell technology [5,6], and (iv) thermoelectric power generation [7]. In many of these applications, the LCO performance is well above that of other perovskite oxides like manganites [3,4,6].

Tailored applications of LCO-related materials rely on a deep comprehension of their physical properties. In the case of LCO, two important modifications of the electronic structure with temperature have been reported: a diamagnetic-to-paramagnetic spin transition (ST) around 100 K and a broad semiconductor-to-metal transition (SMT) between 350 and 650 K. Both transitions are evidenced by changes in magnetic susceptibility, resistivity, atomic structure [8,9], and phonon spectrum [10–12]. In spite of the overall wealth of static studies performed over the years (see Ref. [13] for a review), a unified understanding of the electronic properties of LCO, and in particular of the change of magnetic configuration at the spin transition, is still lacking. Two scenarios have been debated for half a century regarding the origin of the ST: (I) a "low-spin" (LS: t_{2g}^6)–"high-spin" (HS: $t_{2g}^4 e_g^2$) crossover upon thermal excitation with a HS population of 50% at room temperature and long-range order [14–16] and (II) a low-spin–intermediate spin (IS: $t_{2g}^5\ e_g^1$) transition with orbital ordering due to hybridization with the oxygen states [17]. In any case, this one-electron picture might be too simplistic given the d^6 configuration of Co^{3+}. Thus, multiplet calculations for the Co ion in the octahedral crystal field of the oxygen atoms result in a ground state with zero magnetic moment followed by a series of multiplet states with different magnetic moments when the trigonal distortion, intrinsic to the $R\bar{3}c$ rhombohedral structure of the system, and the spin-orbit coupling are taken into account [18]. However, this single-ion description has recently been questioned [19] since the modifications of the crystal field with temperature, which are assumed to be responsible for the transition, rely on a proper description of the hybridization, and requires band-structure calculations. Based on the LDA+DMFT (local density approximation + dynamical mean-field theory) approach, a new vision of the system has been proposed in which Co valence fluctuations are used to explain the changes in hybridization with temperature. This approach provides a description of the system in terms of the LS, HS, and IS configurations. This picture supports the role of dynamic effects in the description of the system that were conjectured a long time ago. Thus, on the basis of the anomalous behavior of the Debye-Waller factor with temperature, Goodenough *et al.* [8] suggested the possible existence of dynamic short-range order with a crossover in the range of 10^{-8} s around 200 K. More recently, fluctuations of orbital order have been proposed to interpret sound velocity propagation experiments [20].

Regarding the SMT crossover, its interpretation relies heavily on the nature of the ST. Up to now, several scenarios remain

to be clarified, including (i) metallization by percolation of domains [8] and (ii) the role played by the oxygen depletion above 600 K remain to be clarified [9,21]. Understanding the SMT crossover is of importance for the optimization of the high-temperature applications of LCO. Disentangling whether metallization is enhanced by oxygen depletion is particularly interesting since it will lead to degradation of LCO-based devices. One interesting approach to investigate the role played by oxygen in the metallization of the system is to excite LCO nonthermally. In this respect, performing pump-probe experiments with a femtosecond optical or x-ray laser pulses is a very promising possibility that should shed light into the significance of dynamics to explain the room-temperature state of the system. Furthermore, we expect ultrashort laser pulses to be able to induce dynamical phase transitions as observed in other systems [22–24], which might lead to new technological possibilities, as recently proposed for high-T_C superconducting oxides [25]. Moreover, LCO is a candidate to exhibit large ionic Raman scattering (IRS), as was recently found in an isostructural manganite $La_{0.7}Sr_{0.3}MnO_3$ (LSMO) [26]. In IRS, the excitation of an infrared-active phonon serves as the intermediate state for the Raman scattering and its origin relies on lattice anharmonicities instead of electron-phonon interactions. In the particular case of LSMO it has been observed that depending on the wavelength of the pump laser, different phonon modes are indirectly excited [26]. More specifically, when using a wavelength in the near infrared and the visible (∼525 nm) the A_{1g} phonon mode at 5.8 THz was excited. In the case of LCO, the corresponding phonon mode resonates at higher frequency (8.7 THz). LCO is semiconducting at room temperature whereas LSMO is metallic, so the coherent oscillations due to excitation of the phonon mode in LCO are expected to be of higher intensity due to a lower screening by free carriers.

In this paper, optical laser pump, soft x-ray reflectivity probe studies on pristine $LaCoO_3$ will be reported in combination with temperature-dependent reflectivity experiments and correlated DFT^{++} theoretical calculations. The comparison between the pump-probe and temperature-dependent reflectivity shows that a transient metallic state, different from the thermally excited one, is induced upon laser excitation. On the other hand, the theoretical results indicate that LCO is better described when the correlations are of the same order of magnitude as the charge transfer. The paper is organized as follows: In Sec. II, the experimental details are provided. In Sec. III, the pump-probe reflectivity spectra at the O K, Co L, and La M absorption edges are discussed together with the temperature data. The response of the system as a function of delay time and fluence is given in Sec. IV. The theoretical calculations within a correlated DFT^{++} are also outlined in Sec. V. Finally, the results are discussed in Sec. VI within the framework of recent experiments and theoretical models before final conclusions and perspectives are provided.

II. EXPERIMENTAL DETAILS

The pump-probe reflectivity experiments were performed at the FEMTOSPEX facilities of the BESSY II storage ring operated by the Helmholtz-Zentrum Berlin [27]. For the dynamical investigations, the output of an amplified Ti:sapphire laser was used as a pump source, and the x-ray photons from the UE56/1-PGM beamline were used as the probe. The laser runs at a maximum repetition rate of 6 kHz with a pulse duration of about 50 fs and a maximum pulse energy of 2 mJ at the fundamental photon energy 1.55 eV ($\lambda = 800$ nm) in a 500-μm diameter spot at the sample position. The laser irradiated area was much larger than the probed part of the samples, since the x-ray beam was focused to a ∼100 μm spot at the sample surface. The pump-probe synchronization was achieved by locking the laser oscillator repetition frequency to the master RF clock of the synchrotron. The probe photons were linearly polarized soft x-rays in the range from 525 to 930 eV with an average resolving power $E/\triangle E \sim 4000$. The time resolution was limited by the duration of the x-ray photon pulses to ∼50 ps, as provided by the single bunch operation mode of the storage ring [28]. The laser and x-ray beams were incident on the sample in a nearly collinear configuration and the reflected x-ray intensity was recorded using a photodiode coupled to a boxcar integrator triggered at the repetition rate of the laser. The experimental geometry was chosen to be $(\theta, 2\theta) = (5^\circ, 10^\circ)$ a compromise between the reflectivity of the sample and the laser spot size and fluence. The spatial and temporal overlap between the pump and probe pulses, as well as the time resolution of the experiment in transmission, was determined from the measurements on a ≈40-nm-thick Ni film. Femtosecond time-resolved x-ray absorption spectroscopy (XAS) measurements of Ni done with the same apparatus have shown the XAS intensity at the L_3 edge to decay within 100 fs [29]. In our case, the decay of the signal was observed to occur within ∼50 ps and was therefore limited by the duration of the single bunch pulse. Note that the temporal resolution varies slightly with time since it scales with the inverse of the current in the storage ring, which was operated in decay mode. The static temperature-dependent reflectivity was measured for s and p polarization in the 273 to 650 K range at the UE56/2-PGM2 monochromator beamline in a dedicated reflectivity chamber. The same sample mounting and preparation were used in order to be able to compare the two sets of data reliably. The use of soft x-ray reflectivity is motivated by the fact that thin films of LCO have different atomic structure to the bulk, which changes the diamagnetic-to-paramagnetic spin transition at low temperatures into a ferromagnetic-to-paramagnetic one [30].

The sample under investigation was a single-crystalline cut obtained from a well-characterized large crystal [31]. The 10×5 mm^2 cut was found to have a 3° misorientation with respect to the (111) low-index surface. The reflectivity measurements were performed at room temperature in a vacuum chamber in the 10^{-8}-mbar pressure range. No further *in situ* cleaning of the sample surface was performed. At the ambient temperature used in the experiments, the sample is semiconducting and the spin configuration according to the model selected is either a mixture of the low-/high-spin state (around 50%-50% composition [14]) or an intermediate-spin configuration with orbital ordering [17]. To obtain a detailed understanding of the system we performed measurements at the O K, Co L, and La M edges of $LaCoO_3$.

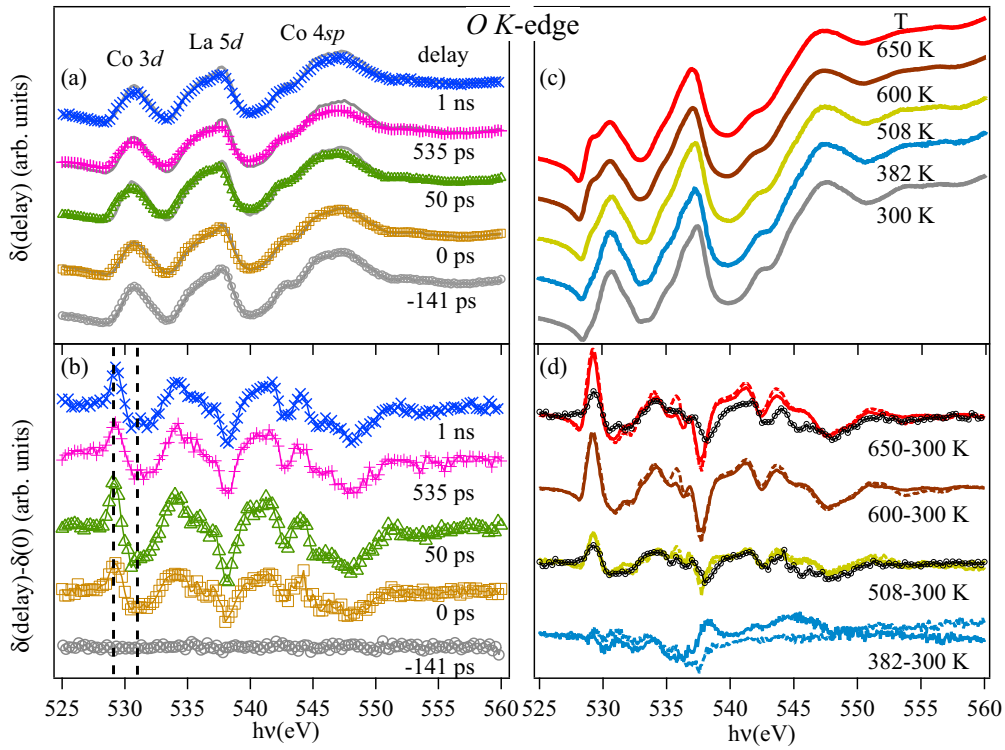

FIG. 1. (Color online) (a) Reflectivity curves taken at the O K edge in the unpumped (solid gray lines) and laser pumped (color marked lines) measurements for different delay times obtained with a maximum laser fluence of 0.43 mJ·cm^{-2}. (b) Difference spectra showing the intensity modifications upon laser pumping for different delays. Three energy regions corresponding to excitation into O 2p empty states hybridized with Co 3d, La 5d, and Co 4sp states are indicated in the figure. (c) Temperature-dependent reflectivity in the range from room temperature to 650 K measured in the same geometrical configuration as the pump-probe data. (d) Thermal reflectivity difference with respect to the 300-K spectra for s and p polarized photons together with the laser-induced reflectivity (black dots).

III. PUMP-PROBE VERSUS TEMPERATURE REFLECTIVITY

Understanding the SMT of LCO with soft x-rays can be accomplished by studying the changes at the O K edge as extracted from XAS studies [15,32]. Changes in the intensity and position of all the features at the edge have been observed. The most significant ones are those at the pre-edge since metallization is supposed to be accompanied by a depopulation of the pseudo-t_{2g} occupied states in favor of the pseudo-e_g ones.[1] As a consequence, intensity modifications at the lowest energy O K pre-edge are expected since these states correspond to O 2p states hybridized with the pseudo-t_{2g} and pseudo-e_g orbitals. Since a change in relative population of the Co 3d orbitals is expected to also modify the spin population the evolution of the Co L edge upon excitation has been also studied in order to understand the effect of the dynamical excitation on the spin state.

In Fig. 1(a), the pump-probe reflectivity data taken at the O K edge for a laser fluence of 0.43 mJ·cm^{-2} are displayed in the energy range from 525.0 to 560.0 eV for different delays. Clear differences between the pumped and unpumped signals are observed for positive delays between the optical laser pump and soft x-ray photons all over the entire edge range, indicating a dynamical state excited upon laser irradiation. In order to better disentangle the modifications upon pumping, the difference signal *Reflectivity(pumped)-Reflectivity(unpumped)* in Fig. 1(a) is plotted in Fig. 1(b). The latter shows that at negative delays no excitation of the system occurs. At zero pump-probe delay, a weak excitation of the system can be seen. It saturates at around 50 ps from where it reduces slightly up to the maximum delay measured (∼1 ns). The temperature-dependent reflectivity in the range from room temperature to 650 K is given in Fig. 1(c) and the difference *Reflectivity(T)-Reflectivity(Room)* in Fig. 1(d) for both s and p polarizations. In the latter, the pump-probe reflectivity difference has also been plotted as black dots for comparison. Since the reflectivity spectra in both sets of measurements were normalized the difference spectra can be directly compared.

The O K edge spectra can be divided in three energy regions: (i) from 527 to 532 eV the intensity is ascribed to excitations from the O 1s filled states into the O 2p empty states hybridized with the Co 3d unoccupied states, (ii) in the 532–539 eV range transitions into the hybridized La 5d states dominate the signal, and (iii) for energies ($h\nu >$ 539 eV) transitions into the hybridized Co 4sp states take place. One can observe that both the laser and thermal

[1]The rhombohedral structure of LCO results in a distortion of the CoO_6 octahedra along the (111) direction that breaks the O_h symmetry. Therefore, the description in term of t_{2g}-e_g orbitals is no longer accurate. Yet, since the distortion is small and mainly lifts the degeneracy of the t_{2g} orbitals, we will describe the changes in terms of pseudo-O_h orbitals as much as possible for simplicity.

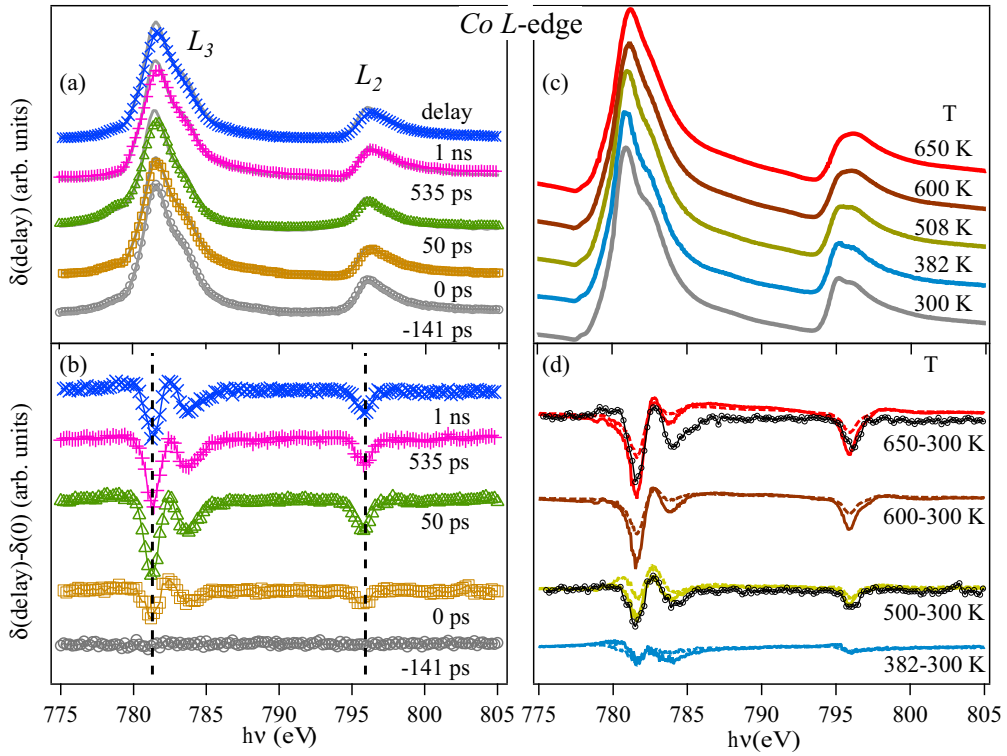

FIG. 2. (Color online) (a) Reflectivity curves taken at the Co L edge in the unpumped (solid gray line) and laser pumped (color marked lines) experiments for different delay times at the maximum laser fluence of 0.43 mJ·cm^{-2}. Difference signals (b) show important intensity modifications upon laser pumping at the L_3 and L_2 white lines, as well as at the shoulder of the L_3 line. (c) Temperature-dependent reflectivity in the range from room temperature to 650 K measured in the same geometrical configuration as the pump-probe data. (d) Thermal reflectivity difference with respect to the 300 K is displayed together with the laser-induced reflectivity (black dots).

excitation of the system result in modifications of the intensity all over the edge, as expected from XAS data [15,32]. An increase of the intensity in the pre-edge region (∼529 eV) is observed for positive time delays in the pump-probe experiments and above 500 K upon static heating, as expected when metallization of the system takes place. The latter is expected due to filling the semiconducting gap and depopulating the t_{2g} orbitals, which are fully occupied in the low-temperature LS state. The La 5d region exhibits only slight intensity modifications upon heating, while in the Co 4sp region the double-peak structure shifts to lower photon energies. These latter changes have been attributed to modifications of bond distances and angles taking place upon metallization [15].

The comparison between the pump-probe and the temperature-dependent data indicates that the dynamical excitation of the system results in metallization of the system at all positive delays. The qualitative spectral shape is similar in both cases, differences can be also determined at the pre-edge, where the signatures of metallization are more significant. From the reflected difference signal at zero delay, the data show variations of the same order of magnitude as the 550-K data in the whole energy range, thus confirming a full metallization of the system at this delay. However, one can observe that the thermal data at the pre-edge exhibit slightly higher intensity. Although one could ascribe the observed difference at the pre-edge to the different energy resolution of the two measurements, the convolution of the temperature-dependent data with a lower resolution function will enhance the intensity differences in the rest of the spectra. For time delays longer than 50 ps, significant differences with respect to the temperature-dependent data can be found in Fig. 1(c). More concretely, the comparison with the maximum temperature (650 K) static data shows similar intensity modifications in the pseudo-t_{eg} and La 5d spectral regions, while noticeable differences are observed at the Co 4sp and pseudo-t_{2g} regions. The magnitude of the differences is very significant in the pseudo-t_{2g} region compared to the thermally activated one and can be understood by assuming a lower depopulation of the pseudo-t_{2g} or a change in the O 2p–Co 3d hybridization upon laser excitation.

The pump-probe reflectivity spectra measured at the Co L edge are displayed in Fig. 2(a) (pumped and unpumped signals) at different delays, and the difference signals are depicted in Fig. 2(b). In Figs. 2(c) and 2(d), the temperature-dependent and difference spectra are given, the latter together with the 0- and 50-ps spectra at the same temperatures as for the O K edge. Like at the O K edge, the pump-probe data show differences at all positive delays with the same time-dependent evolution with a maximum difference at 50 ps. The temperature-dependent data reveal a broadening of the spectra with increasing temperature as expected from XAS experiments [14,15]. Concentrating on the difference spectra, the comparison between the two types of measurements shows that the 0-ps data are almost identical to those around 500 K, except for the shoulder at the high energy of the L_3 white line, which is larger in the pump-probe data. Regarding the 50-ps

data, they show more significant differences with respect to the 650-K case. In particular, while the L_3 and L_2 white line intensity differences have the same order of magnitude between the pump-probe and the temperature data, the pump-probe dynamical difference at the shoulder of the L_3 is significantly enhanced. Furthermore, no dynamical differences are observed at the pre-edge of the L_3 edge, in contrast to the thermal data. Indeed, even the temperature-dependent reflectivity data show a much lower change at the pre-edge compared to the XAS spectra measured simultaneously (not shown). These obvious differences between the pump-probe and the thermal data confirm the results obtained at the O K edge, namely, that the laser induces a transient metallic state different from the thermally excited one. In particular, the modification of the intensity at the high-energy shoulder of the L_3 white line has been related to the increase of the high-spin population in temperature-dependent XAS experiments [14,15]. XAS calculations have shown that an increasing contribution of Co^{3+} in an IS state and/or Co^{4+}, both in a LS or HS population, could also be compatible with an increase of the intensity at this energy [33].

Modifications at the La M edge (not shown) have also been observed at both white lines, indicating that the La atoms also participate actively in the dynamical SMT.

IV. DELAY AND FLUENCE DEPENDENCE

In order to follow the dynamical modifications with higher time precision, reflectivity delay scans with 20-ps time steps were measured at the selected energies of each particular edge for two fluences: 0.20 mJ·cm^{-2} [Fig. 3(a)] and 0.09 mJ·cm^{-2} [Fig. 3(b)]. At the O K edge the photon energy of the pseudo-t_{2g} and pseudo-e_g was measured. At the Co L edge, the intensity at the two white lines was measured, and at the La M edge, the M_5 modifications where measured. The results are displayed in Fig. 3. Aside from the reflectivity on resonance, a spectrum was measured below the Co L edge (gray line) to show that the dynamical modifications only take place at resonances. Furthermore, a delay scan taken for the XAS signal from a ≈40-nm-thick film of Ni is plotted in each panel ("as measured" and inverted) to demonstrate the time resolution of the experiment. The changes in intensity follow those measured in the spectra of Figs. 1 and 2. The changes in the reflectivity difference signal as a function of delay time show a drastic change (drop or increase) at short delay times followed by a slow recovery above 100 ps that stabilizes into a long-living state with little modifications up to the maximum delay measured (∼1 ns). The initial drop in our case is limited by the time resolution available in the experiments, ∼50 ps, as indicated by recent magneto-optical femtosecond pump-probe experiments on LCO thin films [34].

The dynamic excitation of the system for the two different fluences at the selected photon energies for the O K, Co L, and La M edges are plotted separately in Fig. 4. The results show that the behavior as a function of delay time is the same irrespective of the fluence and that only relative intensity variations are observed. In order to quantify them, the average intensity variation at each selected photon energy was determined. Thus, at the O K edge pseudo-t_{2g} the dynamical difference decreases by a factor of 3.42 upon reducing the fluence from 0.20 mJ·cm^{-2} to 0.09 mJ·cm^{-2}. At the La M_5 white line, the relative changes in the reflectivity are larger

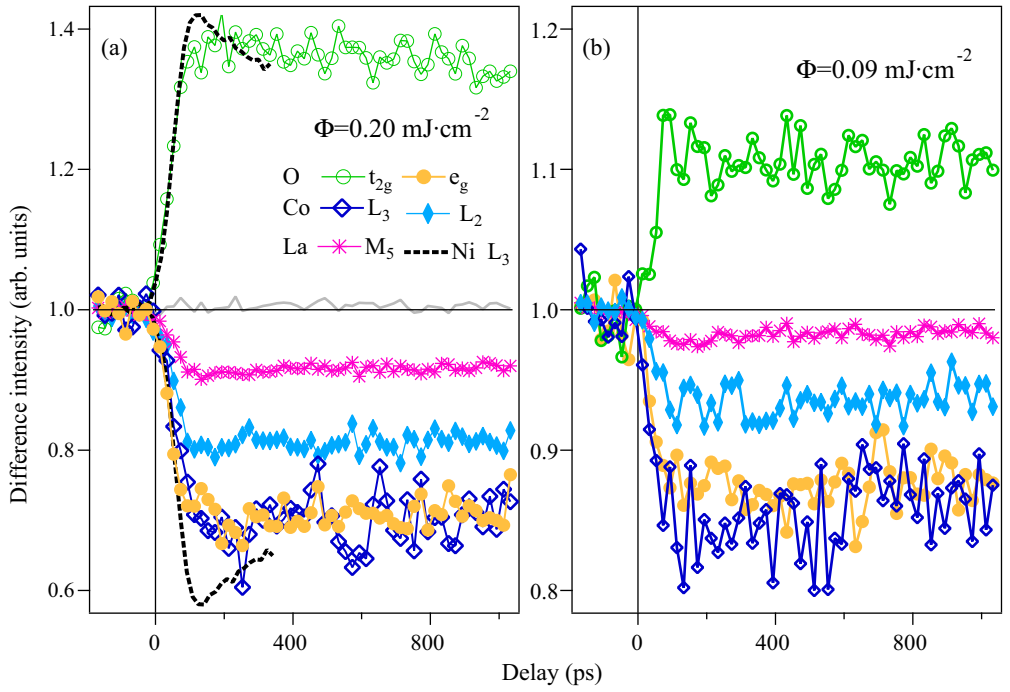

FIG. 3. (Color online) Delay scans taken at the selected photon energies. Two different laser fluence values have been used: 0.20 mJ·cm^{-2} (a) and 0.09 mJ·cm^{-2} (b). For comparison, delay scans are plotted for an ≈40-nm-thick film of Ni as a dashed black line, and for a nonresonant energy (777.0 eV, solid gray line) around the Co L_3 edge. The latter shows no changes with delay time. Qualitatively similar behavior can be observed at both fluences.

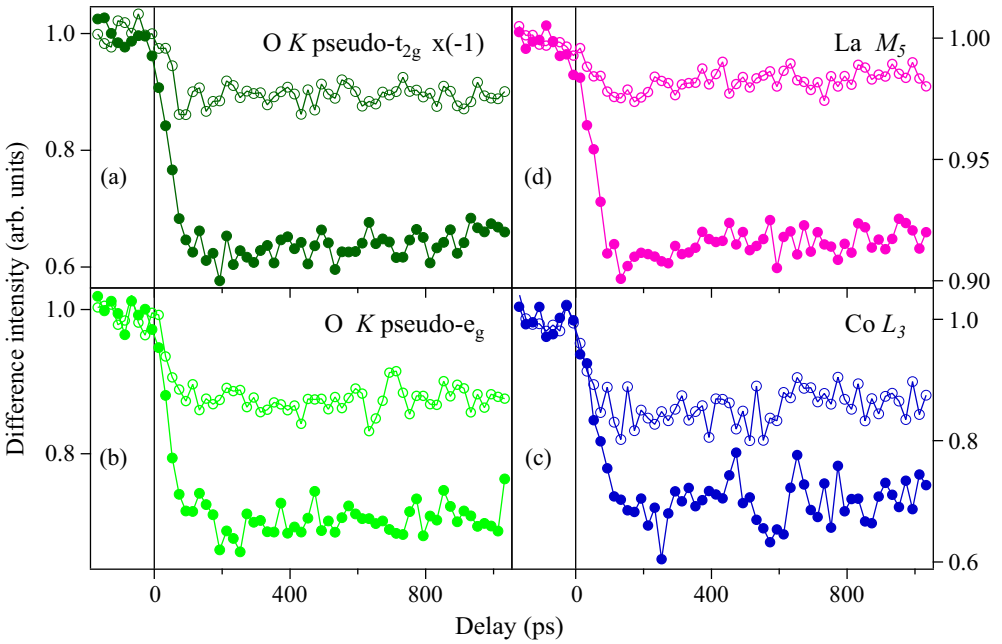

FIG. 4. (Color online) Comparison of the delay scans measured for two different fluences [0.09 mJ·cm^{-2} (open circles) and 0.2 mJ·cm^{-2} (filled circles)] for the pseudo-t_{2g} O K edge (a) and pseudo-e_g (b)], Co L_3 edge (c), and La M edge (d).

(a factor of 4.7). In the case of the O K edge at the e_g region, the change in fluence reduces the dynamical response by a factor of 2.36, which is similar to the value obtained at the Co L_3 edge (a factor of 2.1). These results suggest a correlation between the changes in intensity measured at the O K pseudo-t_{2g} and the La M edges on the one hand, and of the O K pseudo-e_g and Co L edges on the other hand. From the reduction of the intensity at the O pre-edge and the La M edge decrease with laser fluence a threshold fluence of ∼0.04 mJ·cm^{-2} to induce dynamical modifications of these states can be extrapolated. From the O K pseudo-e_g and Co L edges, the threshold was observed at a much lower value of 0.01 mJ·cm^{-2}. In both cases, a linear behavior of the difference reflectivity was assumed. The latter results from a fluence-dependent study performed at the Co L_3 shoulder. The change in reflectivity with fluence was averaged over several pulses and fitted with a line as displayed in Fig. 5.[2]

V. THEORETICAL RESULTS

Since the reported data have shown important deviations from the thermally excited results, theoretical calculations have been performed aiming to understand the properties of the laser excited state. The motivation was twofold: only a few data sets are available for the high-temperature phase of the compound [16]. This is a consequence of the fact that the low-temperature spin transition has been the main focus of investigation of this compound. A second motivation arises from the fact that very often the system has been considered as a strongly correlated *charge-transfer* material with large Coulomb interaction parameter U. Indeed, in the calculations of Korotin *et al.* [17], the IS configuration was stabilized for a U value of 8.0 eV, which resulted in a metallic ground state. The insulating character was then recovered by considering orbital ordering in the system, for which only indirect experimental proofs have been provided so far [20,35]. Posterior LSDA+U calculations in which the influence of U and J (the exchange interaction parameter) were studied have shown that there are a range of U values between 1.5 and 7.0 eV that result in a insulating ground state without requiring orbital ordering [36]. Furthermore, the transitions in the system have been shown to be explicable on solely electronic grounds with an optimal value of $U\sim$ 4.0 eV [16]. This study also pointed out the need for charge disproportionation to fully understand LCO, a finding that is supported by DMFT calculations [19]. The latter results have provided an interpretation of the system in which the LS-HS transition is favored with Co LS and HS

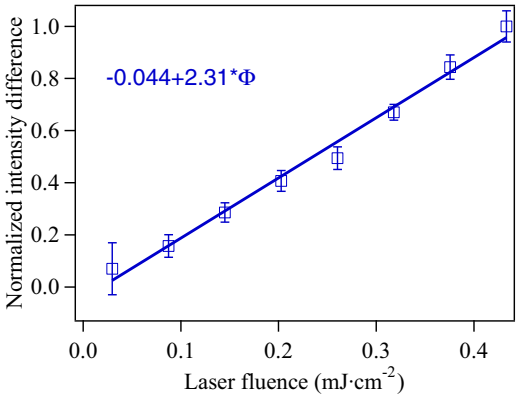

FIG. 5. (Color online) Fluence dependence of the reflectivity difference at the Co L_3 shoulder normalized to the changes at the highest fluence. A linear dependence has been used to fit the data.

[2]A parabolic fit will result in a better fit but without physical value since changes in the reflectivity will be observed at zero fluence.

ions at each side of a Co-O-Co bond, thus requiring short-range local order. A reasonable agreement with photoemission data across the spin transition has also been obtained at the expenses of using different temperatures and lattice structures than the experimental ones. This fact modifies artificially the level of hybridization between orbitals compared to the respective real-temperature structures.

In the context of the above studies and to support the experimental data reported here, calculations have been performed in which the correlations of the Co $3d$ shell beyond Kohn-Sham density-functional theory (DFT) are described using a DFT^{++} approach [37–39]. In this approach, the many-body part was treated within the DMFT formalism (see, e.g. Ref. [40] for a review). The experimental lattice parameter values for the rhombohedral structure were taken from Ref. [9] and the density of states and band structure were calculated using the projector-augmented wave (PAW) based VASP code [41] employing the Perdew-Burke-Ernzerhof (PBE) gradient corrected functional [42]. The PAW basis sets provide intrinsically projections onto localized atomic orbitals [43,44], which have been used to generate the localized basis set for the DFT+DMFT calculations (see Refs. [39,45]). The DMFT calculations were carried out using a finite-temperature exact diagonalization impurity solver [46] employing the Lanczos algorithm [47]. A 10-site cluster (inclusion of an additional bath site per impurity orbital did not alter the results qualitatively) and the full rotationally invariant Coulomb matrix including spin-flip and pair-hopping terms was used to model the system. The calculations were carried out at inverse temperatures $\beta = 40$ eV^{-1} and 15 eV^{-1} for the 300- and 650-K lattices, respectively.

In Fig. 6, the projected density of states (pDOS) at the different O $2p$ and Co $3d$ orbitals is displayed for two temperatures and two different sets of U and J. In Fig. 6(a), the calculation parameters correspond to those used in Ref. [19] ($U = 6.0$ eV and $J = 0.8$ eV), while in Fig. 6(b) the results for smaller values are provided ($U = 3.0$ eV and $J = 0.7$ eV). For any of the two sets of parameters, no closing of the semiconducting gap takes place upon increasing the temperature up to 650 K. However, the top of the occupied states moves with temperature to lower binding energies, as one would expect upon increasing the degree of metallization. These results support a role for charge disproportionation in explaining the metallization of the system that might occur upon oxygen depletion at increased temperatures. Regarding the change of the orbital occupancy and concentrating on the empty states, which are reflected in the XAS and reflectivity spectra, the intensity variations at the pDOS of the pseudo-t_{2g} orbitals of Co have a counterpart in two of the O $2p$ empty orbitals. Similar behavior occurs for the pseudo-e_g orbitals and the remaining O $2p$ orbital, thus proving the well-known hybridization between the O and Co orbitals. This hybridization is independent of the U and J values. However, the filling of the states as a function of the temperature depends very strongly on the particular choice of the parameters. Thus, in the case of $U = 6.0$ eV the changes with temperature are minimal. Actually, the pDOS is in agreement with a HS configuration at both temperatures. The situation is quite different in the case of $U = 3.0$ eV and $J = 0.7$ eV, for which a large redistribution of the spectral weight takes place upon increasing the temperature. More specifically, a large increase of intensity at the lowest-energy features of the O and Co orbitals can be observed when going from 300 to 650 K. Conversely, a decrease of intensity and narrowing of the e_g related pDOS features projected on both O and Co orbitals can be obtained upon decrease of U and J. Similar behavior has been observed for the La $5d$ orbitals (not shown). The observed changes correspond to a change of the spin state of the system from a room-temperature configuration (LS-HS or IS), as can be deduced from the partially filled pseudo-t_{2g} orbitals, to a

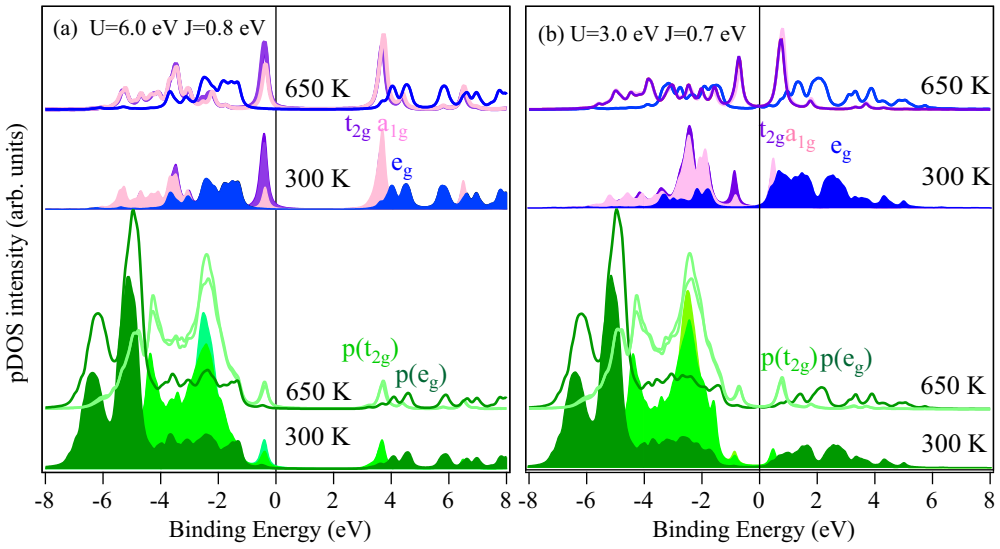

FIG. 6. (Color online) Projected DOS on the Co $3d$ and O $2p$ orbitals obtained for two different values of the Coulomb and exchange potentials: (a) $U = 6.0$ eV and $J = 0.8$ eV as in Ref. [19] and (b) $U = 3.0$ eV and $J = 0.7$ eV. For each set of potentials are results for two different temperatures: 300 and 650 K have been calculated. The lattice parameters of the real structure at the respective temperatures have been taken from Ref. [9] .

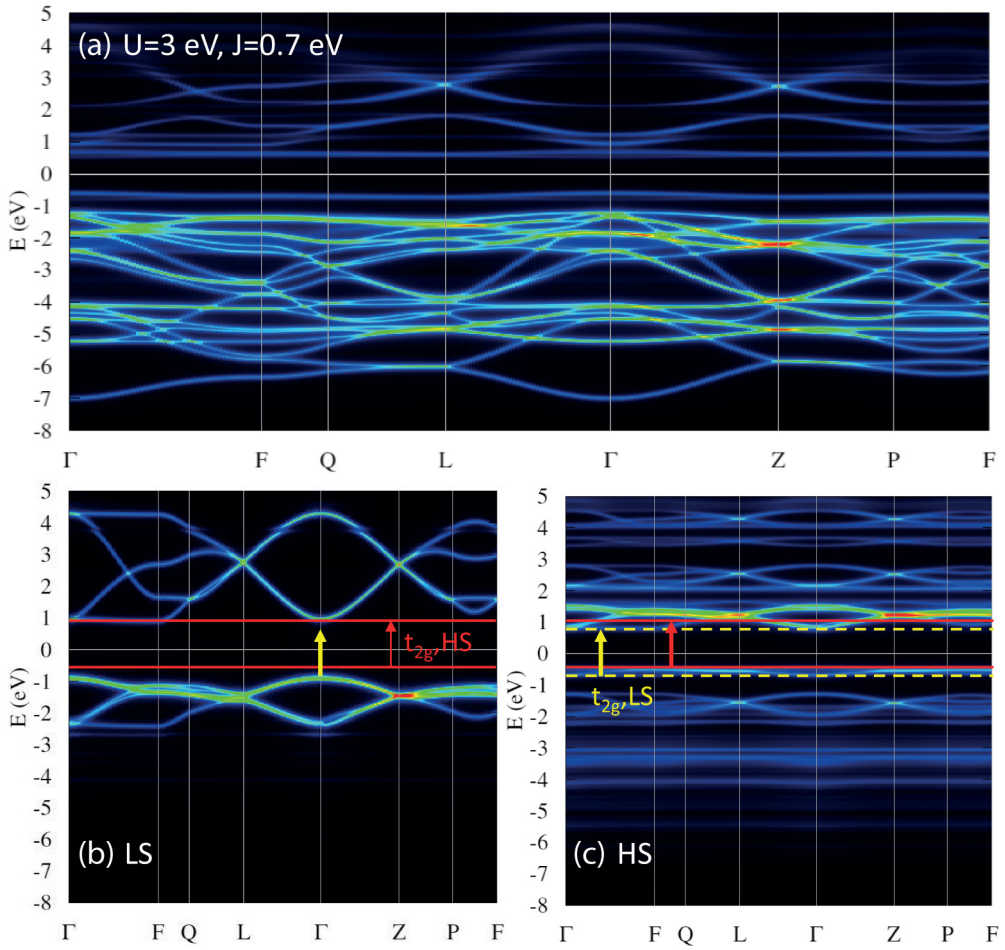

FIG. 7. (Color online) (a) k-resolved band dispersion at room temperature for $U = 3.0$ eV and $J = 0.7$ eV for $LaCoO_3$. The k-resolved dispersion for the pure Co $3d$ states of the low- and high-spin configurations is given in (b) and (c), respectively. Vertical optical transitions with 1.55 eV are also displayed in the latter pictures. For the LS configuration, the photon energy is lower than the intra-atomic pseudo-t_{2g}-e_g energy splitting. On the contrary, the photons can excite transitions to HS pseudo-t_{2g} states. For the high spin, both interatomic and intra-atomic transitions from the pseudo-t_{2g} could be excited.

spin state with higher HS population. This is demonstrated by the increasing depopulation of the pseudo-t_{2g} distorted orbitals upon increasing temperature.

The k-resolved band dispersion at room temperature resulting from the most suitable set of parameters ($U = 3.0$ eV and $J = 0.7$ eV) is displayed in Fig. 7(a). It can be understood as an admixture of LS and HS configurations, displayed in Figs. 7(b) and 7(c). At room temperature, the system is a direct gap semiconductor with a low dispersing state appearing at the top of the valence band due to the high-spin configuration. This state, of pseudo-t_{2g} character, appears as a consequence of the orbital population redistribution taking place in the HS configuration. The energy separation to the lowest conduction band of e_g character is below the laser excitation energy used in this experiment (1.55 eV) along most of the high-symmetry directions. In contrast, only the Γ point of the LS configuration is separated by this amount in the whole Brillouin zone.

VI. DISCUSSION

The performed experiments have shown important differences between the properties of the laser and thermally excited states. The dynamical changes observed upon laser excitation can be seen at all relevant edges including the La M edge. The spectroscopic differences observed between the laser and thermally excited system indicate a laser-induced transient metallic state, as could be anticipated from studies in other systems [22–24].

The experimental observations can be understood in terms of the extensive knowledge acquired over the years in the ultrafast dynamics the physics of semiconductors. Upon femtosecond excitation, several processes are expected with different characteristic time scales. At the initial stage, in the femtosecond time scale, the excitation of carriers and the formation of electron-hole excitons will take place. The latter will thermalize by electron-electron and electron lattice scattering on a subpicosecond and picosecond time scale, respectively. Carrier removal through recombination, Auger, radiative, and diffusion, will take place on longer time scales. These are typically on the nanosecond time scale but can last up to microseconds depending on the system. Finally, thermal effects will take place [48]. Based on this well-known time evolution, the measured delay scans can be understood by assuming that the first drop corresponds to

the carrier excitation and thermalization processes combined. The individual processes are unresolved due to the limited time resolution (∼50 ps) of the experiment. Indeed, recent experiments using femtosecond laser pulses on LCO thin films have shown that the ultrafast carrier excitation takes place in the subpicosecond range and that electron-lattice relaxation has a characteristic time of ∼2.8 ps, which cannot be resolved here [34]. The little recovery observed up to 1 ns indicates that the carrier recombination time in LCO is in the nanosecond range. On the other hand, the time scale used in the experiment results in a homogeneous sampling of the excited state. In fact, the propagation of the excited region into the bulk takes place through coherent acoustic phonon propagation at the speed of sound [49]. For LCO, the longitudinal speed of sound along the (111) direction of the samples is ∼4.124 nm·ps^{-1} [20], which means that even assuming an initial superficial excitation at the surface, the sampled thickness (∼20 nm[3]) will be homogeneously excited in less than 5 ps.

The spectroscopic observation can be interpreted in terms of the transitions excited by the pump laser. At 800 nm (1.55 eV) vertical transitions of the filled pseudo-t_{2g} states into empty pseudo-e_g ones are expected, as proposed by magneto-optical studies on LCO [34,50]. These normally dipolar forbidden dd transitions are allowed through the O $2p$–Co $3d$ hybridization and lattice distortions in the system. Within this ground state, the laser excitation is expected to also reduce the O $2p$–Co $3d$ overlap and consequently the bandwidth. This reduction of the hybridization can explain the smaller changes in reflectivity difference observed in the pseudo-t_{2g} region of the O K edge upon laser excitation. Furthermore, lattice relaxation is also expected to take place on the time scale of the tens of picoseconds. It should therefore be stabilized at the shortest delays used in the experiments and contribute to the differences between the laser and thermally excited sample in the Co $4sp$ energy range of the O K edge.

The changes observed at the Co L edge, can be understood from the hybridization allowed dd transitions. Since they take place from pseudo-t_{2g} to e_g they will result in an overall increase of the high-spin configuration of the system. From the band dispersions obtained for a pure LS and HS configuration displayed in Figs. 7(b) and 7(c) one can see that the photon energy is much lower than the intra-atomic pseudo-t_{2g}-e_g energy splitting of the LS Co atoms. However, transitions to the HS pseudo-e_g are energetically allowed. The laser photons can excite transitions from HS pseudo-t_{2g} states to pseudo-e_g states of the same HS atom or to a LS one. From the energetically allowed transitions, there are several reasons to think that the probability of having these types of vertical transitions should be higher for the HS Co atom to a LS one. These are (i) the dispersion of these spin pseudo-t_{2g} orbitals is quite flat, therefore electrons in extended portions of the reciprocal space can make transitions to pseudo-e_g states with 1.55 eV or less. (ii) The transitions are mediated by hybridization with O $2p$ orbitals, therefore they are expected to be interatomic. (iii) The LS configuration atom has larger covalency with O atoms and therefore transitions to those LS atoms should be more favorable. (iv) LS atoms have all pseudo-e_g states empty and therefore electrons can be excited independently of their spin alignment. These interatomic transitions can be also justified in the current understanding of the system which assumes that at room temperature the population of LS/HS atoms is ∼50% and that one LS and one HS Co atom are present at each side of an O atom [19]. The lack of intensity enhancement at the pre-edge of the Co L edge might be understood by the different, and most likely higher, excited state accessible upon laser pumping compared to the thermally excited one.

Assuming these facts, transitions from HS to LS states would result in an increase of the charge disproportionation and the nominal Co^{3+} configuration will have an increasing contribution from Co^{4+} and Co^{2+} configurations. Contributions from other states can also occur if one takes into account that charge disproportionation is already present at room temperature [19]. The excited states will have also a HS configuration since pseudo-t_{2g} electrons are removed from one site and e_g populated at the other. From cluster calculations of XAS spectra of CoO_6 in different charge and spin configurations [33], one can see that the large increase of the intensity at the high-energy side of the L_3 edge is compatible with an increased presence of Co^{4+} atoms. This high-energy contribution is the dominant feature of the spectra. The low-energy feature, below the L_3 white line, that should also be present is of much lower intensity and cannot be seen in our data. Likewise, we see no contribution of the Co^{2+} states in a HS configuration also expected at this energy. This might be explained because the Co^{2+} ionic radius is much larger (∼0.7 pm) than the Co^{3+} (0.545, 0.560, and 0.61 pm for the LS, IS, and HS configurations) and the Co^{4+} one which has to be smaller than for the the Co^{3+} ion. As a consequence, the oxygen octahedra should be distorted, resulting in a change of the spectrum. The change of the ionic radius expected upon increasing charge disproportionation might be able to explain the changes in atomic distortions through lattice relaxation. In fact, a distortion of the O octahedra around the Co atoms should also affect the La atoms, therefore explaining their role in the laser-induced metallization. The different change in the ionic radius of the excited Co ions is expected to result in two inequivalent octahedral environments. This fact might also have an impact on possible coherent phonon excitations due to ionic Raman scattering in the system. Although expected from experiments in isostructural manganites [26], it has not been observed in LCO so far [34]. This could be due to the different environment of the LS and HS Co^{3+} configurations due to their different ionic radii. The difference will be enhanced upon laser excitation assuming an increase of charge disproportionation with even larger increase in ionic radius differences. In any case, the time resolution of the experiment is not enough to observe them since they should appear at a frequency of 8.7 THz which corresponds to 0.114 ps.

From the analysis of the fluence dependence, the existence of two fluence thresholds was derived. One for the excitation in the region of the white line of the Co L edge and the pseudo-e_g of the O K edge at ∼ 0.01 mJ·cm^{-2} and a higher one at ∼0.04 mJ·cm^{-2} required to induce dynamical changes in the region of the white line

[3]The sampled thickness of the x rays has been estimated from the saturation effects observed in XAS at the grazing geometry used in the experiment compared to normal incidence measurements.

of the La M edge and the low-energy region of the O K edge. The former would correspond to the minimum fluence required to induce changes in the spin population, whereas the latter relates to the minimum fluence necessary to achieve metallization, which will induce further changes in the spin population.

VII. CONCLUSIONS

The dynamical response of $LaCoO_3$ single crystals upon excitation with 800-nm fs pulses was studied by means of pump-probe and temperature-dependent soft x-ray reflectivity measurements and theoretical calculations within a DFT^{++} formalism to take into electron correlations. It was found that modifications of the reflectivity spectra are induced at absorption edges of all the atomic species present in the compound. The spectroscopic modifications show mainly intensity variations with laser fluence within the time resolution available. Quantitatively, the dynamical changes observed as a function of fluence at the O K pre-edge and La M edges indicate that these two species participate actively in the laser-induced metallic state. On the other hand, the spin-related modifications at the O K edge in the pseudo-e_g and the Co L edges follow a similar dependence with fluence. The spectral shape of the pump-probe reflectivity differs strongly from that measured as a function of the temperature, indicating a dynamically induced transient metallic state with larger high-spin content and charge disproportionation induced by the optical excitation.

ACKNOWLEDGMENTS

The authors would like to acknowledge N. Pontius and C. Schüessler-Langeheine for their efficient support during experiments, to R. Carley for his native proofreading to improve the manuscript, and the interesting discussions with him and A. Scherz during its preparation. This project, currently supported by the BMBF Proposal No. 05K12GU2, was initiated within the framework of a scientific collaboration between the European XFEL and Synchrotron Soleil. M.I. acknowledges both institutions for financial and scientific support of this initiative. Financial support by the Deutsche Forschungsgemeinschaft through SFB 668 is gratefully acknowledged.

[1] N. Li, A. Boréave, J.-P. Deloume, and F. Gaillard, Solid State Ionics **179**, 1396 (2008).
[2] M. Alifanti, J. Kirchnerova, B. Delmon, and D. Klvana, Appl. Catal., A **262**, 167 (2004).
[3] C. H. Kim, G. Qi, K. Dahlberg, and W. Li, Science **327**, 1624 (2010).
[4] O. Büchler, J. Serra, W. Meulenberg, D. Sebold, and H. Buchkremer, Solid State Ionics **178**, 91 (2007).
[5] M. C. Álvarez-Galván, D. A. Constantinou, R. M. Navarro, J. A. Villoria, J. L. G. Fierro, and A. M. Efstathiou, Appl. Catal., B **102**, 291 (2011).
[6] Y. L. Lee, J. Kleis, J. Rossmeisl, and D. Morgan, Phys. Rev. B **80**, 224101 (2009).
[7] A. A. Taskin, A. N. Lavrov, and Y. Ando, Phys. Rev. B **73**, 121101 (2006).
[8] P. M. Raccah and J. B. Goodenough, Phys. Rev **155**, 932 (1967).
[9] P. G. Radaelli and S.-W. Cheong, Phys. Rev. B **66**, 094408 (2002).
[10] S. Yamaguchi, Y. Okimoto, and Y. Tokura, Phys. Rev. B **55**, R8666 (1997).
[11] Y. Kobayashi, T. S. Naing, M. Suzuki, M. Akimitsu, K. Asai, K. Yamada, J. Akimitsu, P. Manuel, J. M. Tranquada, and G. Shirane, Phys. Rev. B **72**, 174405 (2005).
[12] N. Orlovskaya, D. Steinmetz, S.Yarmolenko, D. Pai, J. Sankar, and J. Goodenough, Phys. Rev. B **72**, 014122 (2005).
[13] N. B. Ivanova, S. G. Ovchinnikov, M. M. Korshunov, I. M. Eremin, and N. V. Kazak, Phys. Usp. **52**, 789 (2009).
[14] M. W. Haverkort, Z. Hu, J. C. Cezar, T. Burnus, H. Hartmann, M. Reuther, C. Zobel, T. Lorenz, A. Tanaka, N. B. Brookes *et al.*, Phys. Rev. Lett. **97**, 176405 (2006).
[15] M. Abbate, J. C. Fuggle, A. Fujimori, L. H. Tjeng, C. T. Chen, R. Potze, G. A. Sawatzky, H. Eisaki, and S. Uchida, Phys. Rev. B **47**, 16124 (1993).
[16] J. Kuneš and V. Křápek, Phys. Rev. Lett. **106**, 256401 (2011).
[17] M. A. Korotin, S. Y. Ezhov, I. V. Solovyev, V. I. Anisimov, D. I. Khomskii, and G. A. Sawatzky, Phys. Rev. B **54**, 5309 (1996).
[18] Z. Ropka and R. Radwanski, Phys. B (Amsterdam) **312–313**, 777 (2002).
[19] V. Křápek, P. Novák, J. Kuneš, D. Novoselov, D. M. Korotin, and V. I. Anisimov, Phys. Rev. B **86**, 195104 (2012).
[20] T. S. Naing, T. Kobayashi, Y. Kobayashi, M. Suzuki, and K. Asai, J. Phys. Soc. Jpn. **75**, 084601 (2006).
[21] G. Vankò, J.-P. Rueff, A. Mattila, Z. Németh, and A. Shukla, Phys. Rev. B **73**, 024424 (2006).
[22] M. Rini, R. Tobey, N. Dean, J. Itatani, Y. Tomioka, Y. Tokura, R. W. Schoenlein, and A. Cavalleri, Nature (London) **449**, 72 (2007).
[23] A. Cavalleri, Nat. Photonics **5**, 506 (2011).
[24] A. Dienst, M. C. Hoffmann, D. Fausti, J. C. Petersen, S. Pyon, T. Takayama, H. Takagi, and A. Cavalleri, Nat. Photonics **5**, 485 (2011).
[25] M. Gabay and J. M. Triscone, Nat. Photonics **5**, 447 (2011).
[26] M. Foerst, C. Manzoni, S. Kaiser, Y. Tomioka, Y. Tokura, R. Merlin, and A. Cavalleri, Nat. Phys. **7**, 854 (2011).
[27] K. Holldack, J. Bahrdt, A. Balzer, U. Bovensiepen, M. Brzhezinskaya, A. Erko, A. Eschenlohr, R. Follath, A. Firsov, W. Frentrup *et al.*, J. Synchrotron Rad. **21**, 1090 (2014).
[28] M. Abo-Bakr, J. Feikes, K. Holldack, G. Wüstefeld, and H. W. Hübers, Phys. Rev. Lett. **88**, 254801 (2002).
[29] C. Stamm, T. Kachel, N. Pontius, R. Mitzner, T. Quast, K. Holldack, S. Khan, C. Lupulescu, E. F. Aziz, M. Wietstruk *et al.*, Nat. Mater. **6**, 70 (2007).
[30] D. Fuchs, E. Arac, C. Pinta, S. Schuppler, R. Schneider, and H. v. Löhneysen, Phys. Rev. B **77**, 014434 (2008).
[31] D. Prabhakaran, A. Boothroyd, F. Wondre, and T. Prior, J. Cryst. Growth **275**, e827 (2005).

[32] Z. Hu, H. Wu, T. C. Koethe, S. N. Barilo, S. V. Shiryaev, G. L. Bychkov, C. Schüssler-Langeheine, T. Lorenz, A. Tanaka, H. H. Hsieh *et al.*, New J. Phys. **14**, 123025 (2012).
[33] M. Merz, P. Nagel, C. Pinta, A. Samartsev, H. v. Löhneysen, M. Wissinger, S. Uebe, A. Assmann, D. Fuchs, and S. Schuppler, Phys. Rev. B **82**, 174416 (2010).
[34] J. Bielecki, A. D. Rata, and L. Börjesson, Phys. Rev. B **89**, 035129 (2014).
[35] G. Maris, Y. Ren, V. Volotchaev, C. Zobel, T. Lorenz, and T. T. M. Palstra, Phys. Rev. B **67**, 224423 (2003).
[36] Z. Yang, Z. Huang, L. Ye, and X. Xie, Phys. Rev. B **60**, 15674 (1999).
[37] A. I. Lichtenstein and M. I. Katsnelson, Phys. Rev. B **57**, 6884 (1998).
[38] V. I. Anisimov, A. I. Poteryaev, M. A. Korotin, O. A. Anokhin, and G. Kotliar, J. Phys.: Condens. Matter **9**, 7359 (1997).
[39] M. Karolak, T. O. Wehling, F. Lechermann, and A. I. Lichtenstein, J. Phys.: Condens. Matter **23**, 085601 (2011).
[40] A. Georges, G. Kotliar, W. Krauth, and M. J. Rozenberg, Rev. Mod. Phys **68**, 13 (1996).
[41] G. Kresse and J. Hafner, J. Phys.: Condens. Matter **6**, 8245 (1994).
[42] J. P. Perdew, K. Burke, and M. Ernzerhof, Phys. Rev. Lett. **77**, 3865 (1996).
[43] P. E. Blöchl, Phys. Rev. B **50**, 17953 (1994).
[44] G. Kresse and D. Joubert, Phys. Rev. B **59**, 1758 (1999).
[45] B. Amadon, F. Lechermann, A. Georges, F. Jollet, T. O. Wehling, and A. I. Lichtenstein, Phys. Rev. B **77**, 205112 (2008).
[46] M. Caffarel and W. Krauth, Phys. Rev. Lett. **72**, 1545 (1994).
[47] M. Capone, L. de Medici, and A. Georges, Phys. Rev. B **76**, 245116 (2007).
[48] S. K. Sundaram and E. Mazur, Nat. Mater. **1**, 217 (2002).
[49] Y. Okimoto, X. Peng, M. Tamura, T. Morita, K. Onda, T. Ishikawa, S. Koshihara, N. Todoroki, T. Kyomen, and M. Itoh, Phys. Rev. Lett. **103**, 027402 (2009).
[50] S. Yamaguchi, Y. Okimoto, K. Ishibashi, and Y. Tokura, Phys. Rev. B **58**, 6862 (1998).